Available online at www.sciencedirect.com

ScienceDirect

Energy Procedia 55 (2014) 190 – 196

Energy Procedia

4th International Conference on Silicon Photovoltaics, SiliconPV 2014

Application of a silicon nanocrystal down-shifter to a c-Si solar cell

Stefan L. Luxembourg[a,*], Antonius R. Burgers[a], Rens Limpens[b], Tom Gregorkiewicz[b] and Arthur Weeber[a]

[a]*ECN Solar Energy, P.O. Box 1, 1755ZG Petten, The Netherlands*
[b]*VanderWaals – Zeeman Institute, University of Amsterdam, Sciencepark 904, 1098XH Amsterdam, The Netherlands*

Abstract

Silicon nanocrystals (Si NCs) in a matrix of SiO_2 were applied to the front of a p-type c-Si solar cell as down-shifter. The down-shifting action of the Si NCs was confirmed from the analysis of spectral response measurements with the help of ray tracing simulations. Ray tracing simulations were performed to simulate the application of a Si NC layer with varying emission quantum efficiencies to the glass coversheet in a solar module with EVA as encapsulant. It is found that gain in J_{sc} is only achieved for a Si NC layer with high emission quantum efficiencies, which requires efficient quantum cutting. The most important loss factors identified are the low Si NC emission coupling efficiency in combination with parasitic absorption in the spectral range of high solar cell internal quantum efficiency.

Peer-review under responsibility of the scientific committee of the SiliconPV 2014 conference

Keywords: Spectral conversion; silicon nanocrystals; solar cell

1. Introduction

Spectral conversion aims at improvement of the conversion efficiency of solar cells through modification of the incident solar spectrum to match the spectral range of high quantum efficiency. Several spectral conversion concepts exist: *e.g.* up- and down-conversion and down-shifting [1, 2]. In the process of up-conversion two sub-bandgap photons are combined to yield one above bandgap photon, while in down-conversion (or quantum cutting) one high-energy photon is split into two low-energy (above bandgap) photons. These concepts can potentially raise the

* Corresponding author. Tel.: +31-88-5158256; fax: +31-88-5158214.
E-mail address: luxembourg@ecn.nl

Peer-review under responsibility of the scientific committee of the SiliconPV 2014 conference
doi:10.1016/j.egypro.2014.08.115

efficiency of single junction solar cells above the Shockley-Queisser limit [3]. Finally, down-shifting transforms the high energy of an incoming UV or blue photon to a lower value, which facilitates more efficient carrier collection by reduction of recombination losses at the front of the solar cell and prevention of parasitic absorption. For mc-Si cells it was estimated that down-shifting can result in an efficiency gain of $10\%_{rel}$ [1]. Silicon nanocrystals (Si NCs) show great potential for application as spectral shapers. [4, 5] Due to quantum confinement their optical characteristics can be tuned to yield efficient emission in the near infrared where the c-Si solar cell's internal quantum efficiency (IQE) is highest, while absorption is mainly restricted to the spectral range of low IQE: the blue – UV part of the spectrum [6]. In this study we applied a thin film sample containing Si NCs in a matrix of SiO_2 as down-shifter to a p-type mono-crystalline solar cell with full Al BSF. The effect of the Si NCs on the spectral response of the solar cell / module stack is measured and interpreted with the help of an optical ray tracing model which includes Si NC absorption and emission. In addition, the model is used to simulate the application of a Si NC layer to the module's front glass sheet. In this configuration the application of Si NCs may reduce / prevent parasitic absorption in the anti-reflective coating (ARC) and the module's encapsulant.

2. Experimental and ray tracing simulations

A 400 nm thick a-SiO_x thin film, which was used as seed layer for the NC formation, was grown using a RF magnetron co-sputtering method on a 0.5 by 1.5 cm, 500 µm thick fused silica (FS) substrate. NC formation was achieved through high temperature annealing at 1250 ^oC; subsequently a low temperature annealing step at 450 ^oC in H_2 atmosphere was performed to improve surface passivation [7]. In this study the SiO_2/Si NC sample was applied to a p-type c-Si solar cell with pyramidal front surface texture, a-SiN_x:H anti-reflective coating and full Al BSF.

The n, k values of the SiO_2/Si NC layer were estimated from R,T measurements of the thin film on the FS substrate using a spectrophotometer which incorporates an integrating sphere. Subsequently, the measured data were fit using an in-house designed optical stack model to obtain the n, k-data.

Si NC emission quantum efficiencies were measured in an integrating sphere with a Xenon lamp as excitation source coupled to an MSA-130 monochromator, produced by Solar Laser Systems. Detection was performed with a M266 monochromator, also manufactured by Solar Laser Systems, coupled to a Hamamatsu CCD (type:C7557-01). Photoluminescence spectra were recorded with the same detection system and a Nd:YAG laser pumped OPO system (Solar Laser Systems), having a frequency of 100 Hz and a pulse width of 5 ns, as excitation source.

Spectral response measurements were performed in the range between 300 and 1100 nm on an Optosolar set-up with a spot size of approximately 1 mm in diameter, which could be positioned between the solar cell's fingers. Measurements were performed on the bare solar cell in air and on module like structures. The latter structures were prepared by masking the solar cell's surface except for an area of 0.5 by 1 cm where the 500 µm thick FS substrate with or without the SiO_2/Si NC thin film was placed. Underneath the FS substrate a droplet of refractive index matching liquid (RIML) obtained from Cargille Laboratories (Cedar Grove, USA) was applied. The resulting structure closely resembles the optical configuration present in a solar module. The RIML's refractive index matches that of FS. The SiO_2/Si NC sample was positioned with the NCs directed towards the cell. The SR data were converted to External Quantum Efficiencies (EQE) of the measured structures.

For our optical simulations we apply 3-D geometrical ray tracing. [8] The simulated structure consists of a FS substrate (or glass coversheet), the SiO_2/Si NC layer, the RIML (or encapsulant) and the solar cell, including SiN_x ARC, silicon wafer material (200 µm thickness) with front pyramidal texture (54.74^o base angle) and Al back reflector. The back surface reflection is parameterized with a fixed reflection of 80% and pyramidal texture with characteristic angle of 10^o. It was found that these parameters gave the best fit of the cell's escape reflectance.

Rays of different wavelengths are shone onto the device structure, and they are traced through the structure. A ray is followed until it is absorbed, *e.g.* in the bulk of the silicon where it can contribute to the current or in one of the other layers resulting in parasitic absorption, or it escapes the system at the front side (reflection by the structure) or it escapes at the rear side (transmission by the structure). The model uses the Fresnel's equations and the transfer matrix method to determine reflection and transmission at interfaces, taking into account interference coatings and the properties of metals and dielectrics.

Random numbers are used to determine the path of the ray whenever it can follow multiple tracks. *E.g.* suppose at an interface between two media a ray has 10% probability of being reflected, and 90% of being transmitted. A

random number r is then drawn from a uniform distribution in the interval [0,1]. If r < 0.1 we assume the ray is reflected, if r >= 0.1 the ray is transmitted. Due to the statistical nature of the method, a sufficient number of rays has to be shone on the structure to obtain sufficiently accurate results. The QE of the Si NC layer is treated analogously. When a ray is absorbed in the Si NC layer by a quantum dot, we draw a random number r from a uniform distribution in the interval [0,1]. Suppose the QE is 80%, if r < 0.8 we assume the ray is absorbed and emitted, if r >= 0.8 the ray is absorbed, but not emitted. Once we have established that the ray is emitted, we need to determine an emission wavelength. The emission spectrum is interpreted as a probability distribution. A random wavelength is selected from this distribution, and, in case the absorption and emission spectra overlap, the additional constraint that the emission wavelength must be larger than the original wavelength applies. Si NC emission is assumed to be isotropic.

From the ray tracing simulations optical parameters such as the absorption in the silicon base material (A_{Si}), total reflection, SiN_x absorption, Si NC absorption and emission, etc. can be determined. The simulated A_{Si} is subsequently used to calculate the EQE, according to:

$$EQE = IQE_{sim} \times A_{Si} \tag{1}$$

IQE_{sim} is derived from the experimentally determined IQE (IQE_{exp}) for the bare solar cell and refers to the efficiency with which photons which are absorbed in the Si can generate collectable charge carriers. Thereby, it differs from the IQE_{exp} which is lowered by parasitic absorption in the ARC, the metal back reflector and in the doped regions. IQE_{sim} has to be corrected for this, which is done in the following way:

$$IQE_{sim} = \frac{IQE_{\exp}}{A_{Si}} \times (1 - R_T) \tag{2}$$

Where R_T corresponds to the sum of front surface and escape reflection, as determined from ray tracing simulations of the solar cell in air.

In the case Si NCs are present in the simulated structure A_{Si} contains contributions from the absorption of rays which are transmitted by the Si NC layer as well as rays which are down-shifted by the Si NCs. The total EQE consists of the sum of the EQE due to the transmitted rays and the EQE due to the absorbed and down-shifted rays, which can be obtained separately from the simulations.

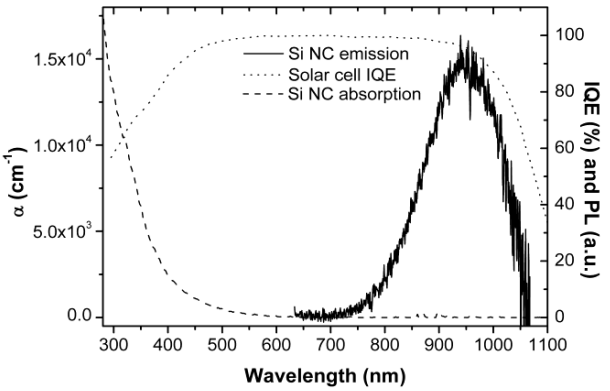

Fig. 1 Absorption and emission spectra of the SiO_2/Si NC sample plotted together with the IQE of the p-type c-Si solar cell used in this study.

3. Results

In Figure 1 the absorption and emission spectra of the SiO_2/Si NC thin film are shown together with the IQE spectrum of the p-type c-Si solar cell, which was used in this study. Clearly, the spectral range where the Si NC absorption shows a steep increase overlaps with the cell's low IQE range. The emission of the Si NC sample used in this study is centered around 950 nm and is therefore predominantly in the range of high IQE. Its photoluminescence quantum efficiency ($QE_{Si\ NC}$) was determined to be approximately 17% (data not shown). The refractive index of the SiO_2/Si NC layer was determined to be close to 1.6 in the wavelength range of NC emission. The EQEs of three different structures were determined: 1) bare solar cell in air, 2) solar cell / RIML / FS substrate and 3) solar cell / RIML / Si NC layer / FS substrate. In the following these will be referred to as S1, S2 and S3, respectively. The results are shown in Figure 2. S2 and S3 were prepared as explained in the experimental section. The structure obtained by the application of the RIML has clear parallels with the optical layer stack in a solar module (Fig. 2a). The refractive index of the RIML matches that of FS. As opposed to the situation where one would leave an air gap between the FS substrate and the front surface of the solar cell its application reduces reflection of incident light and improves coupling of the Si NC emission to the solar cell. As can be seen in Fig. 2b the application of the RIML and the FS substrate results in a reduction of the EQE for wavelengths above 450 nm. This is due to the extra reflection at the air-FS interface. Below 450 nm the anti-reflective properties of the SiN_x coating are improved in the presence of the RIML. The application of the Si NC layer (S3) results in a decrease in the EQE with respect to S2 due to the absorption by the Si NCs starting around 650 nm. This observation is in line with expectations since above 450 nm the EQE of S2 is around 90% and therefore much larger than $QE_{Si\ NC}$. For lower wavelengths the difference between $QE_{S\ NC}$ and the EQE of S2 (and S1) is reduced. Though, as the absorption in the Si NC layer increases steeply here, the EQE of S3 drops further below the EQE of S2. In addition to the low $QE_{Si\ NC}$, the mismatch in refractive indexes of the RIML (n=1.46) and SiO_2 Si NC layer (n=1.6) results in a low coupling efficiency of the NC emission.

As explained in the experimental section a ray tracing model was set up to further investigate the potential of the application of Si NCs to the module glass of a c-Si solar module. The experimentally determined optical parameters of the SiO_2/Si NC layer are included in the model. The measurements were compared with the outcome of the simulations. With the model the contribution of the Si NC emission to the EQE of the total stack can be obtained. In figure 3a measured and simulated data for S2 and S3 are included, while in Figure 3b the contribution of the Si NC emission to the total EQE of S3 is shown. It is evident that the simulations can reproduce the measured EQE spectra. Nevertheless, in the UV as well as the NIR parts of the spectra there is a slight mismatch between the measured and simulated data. For both S2 and S3 the simulations underestimate the response in the NIR. Most probably this arises from an imperfect parameterization of the back reflector in the current version of the model, which leads to a (slight)

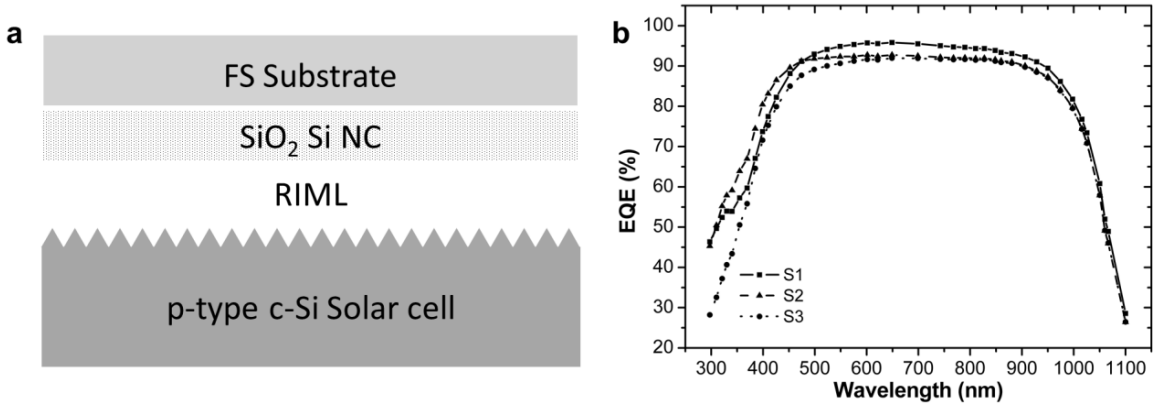

Fig. 2 (a) Schematic representation of the solar cell stack used in the SR measurements. This structure was defined in the ray tracing software for simulations (see text); (b) The EQE curves obtained from the SR measurements.

underestimation of A_{Si}. Since, the NC emit in the NIR this also leads to an underestimation of the EQE of S3 in the UV where the Si NC absorb. From the simulations, the Si NC contribution to the EQE ($EQE_{Si\ NC}$) is found to be 2.6% at 300 nm for a $QE_{Si\ NC}$ of 17%. We conclude that in order to simulate the EQE of S3 correctly down-shifting action of the Si NCs should be taken into account.

Next the ray tracing model was used to access the potential of the application of Si NCs as down-shifting layer on the back of the glass coversheet in a (p-type) c-Si module as well as the factors which determine if gain in J_{sc} can be realized. For this purpose the $QE_{Si\ NC}$ is set equal to 1 and the emission spectrum of the SiO_2/Si NC layer (Fig. 1) is blue shifted by 100 nm. The current full Al BSF cell has a rather low response in the NIR due to a relatively high backsurface recombination and absorption in the metal. Therefore, this shift improves overlap of the emission with the solar cell's high IQE region. In addition, this approach diminishes the effect of the imperfections in the simulation of the Al back reflector. Since there are reports in literature [9] where the Si NC emission has been tuned in this range this seems a valid approach. In order for the simulations to resemble the module's optical stack the FS substrate was replaced by glass and the RIML by EVA in the structure of Fig. 2a. In order to enable high transmission in the UV part of the spectrum the simulations were performed with PPG's low iron Starphire® glass as coversheet with a thickness of 3.2 mm. N, k data were obtained from the PV Lighthouse website [10]. To increase Si NC absorption the SiO_2/Si NC layer thickness was chosen at 1 μm. The EVA thickness was set at 450 μm, which is a typical thickness in a module. The EQE spectra of the resulting module stack with and without the Si NC layer are shown in Fig. 4a. Due to the strong UV absorption in the EVA the EQE of the stack without Si NCs decreases rapidly below 400 nm. Clearly, below 375 nm the absorption and efficient emission by the Si NCs results in a gain of the EQE with respect to the module without Si NCs. Initially, there is an increase in EQE towards the UV part of the spectrum, but absorption in the glass reduces this again further in the UV. Although, the $QE_{Si\ NC}$ is equal to 1, between 400 and 600 nm the Si NC absorption results in a decrease in quantum efficiency. This is a consequence of the low coupling efficiency of the NC emission with the solar cell when EVA is present as encapsulant. The low coupling efficiency results from the fact that part of the emitted light will undergo total internal reflection at the interface between EVA and the SiO_2/Si NC layer. Since the refractive index of the SiO_2/Si NC layer in the NIR is just below 1.6 and the refractive index of EVA is around 1.47 the critical angle is around 65^o. As a consequence a significant part of the emitted photons undergo total internal reflection. In addition, another significant fraction will exit the structure at the front of the module stack. From the ray tracing simulations it was found that 52.8% of the emitted photons will reach the solar cell. Overall the application of the Si NC layer results in a decrease of the J_{sc} of 0.28 $mA \cdot cm^{-2}$ under AM 1.5 illumination, which corresponds to approximately 0.8% of the total J_{sc}. In Table 1 an overview is given of the Si NC contribution to J_{sc} for a $QE_{Si\ NC}$ of 1 and a layer thickness of 1 μm and of the loss processes limiting the Si NC contribution to the EQE.

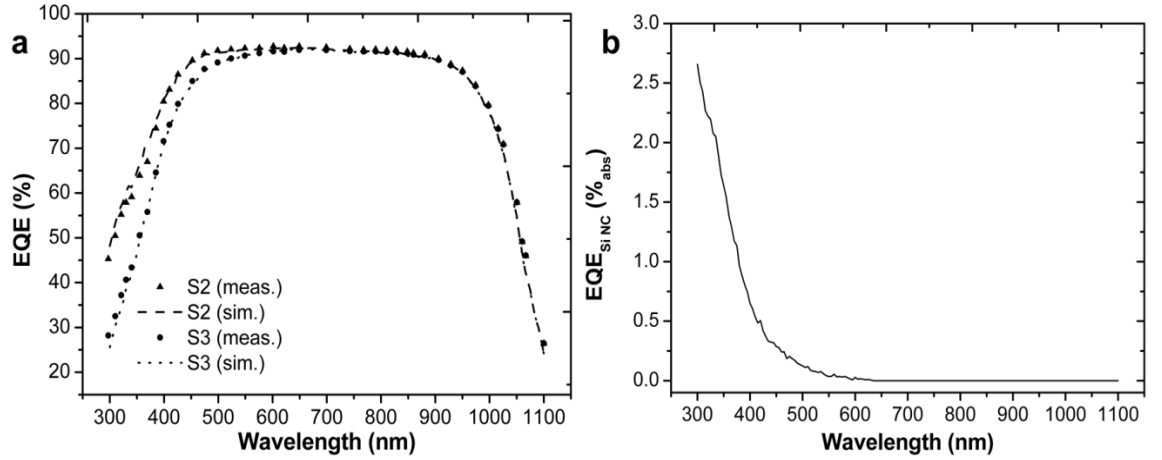

Fig. 3 (a) The experimentally determined EQE of the solar cell/RIML/FS substrate stack and the configuration containing he Si NC layer are accurately reproduced in the raytracing simulations; (b) From the validated the model Si NC contribution to the total EQE was isolated. It follows the Si NC absorption.

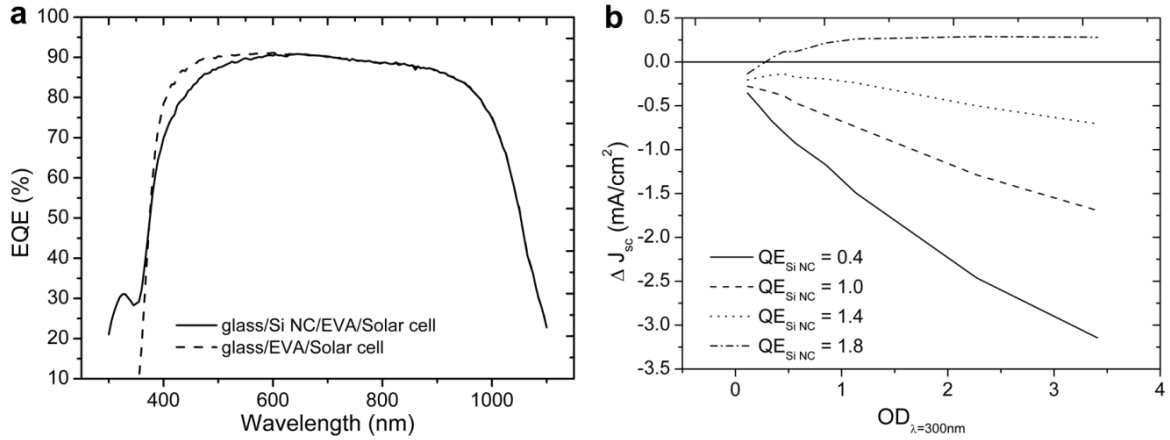

Fig. 4 (a) Comparison of the simulated EQEs of module stacks with and without Si NC layer. The thickness of the Si NC layer is set at 1 μm and $QE_{Si\ NC}$ at 1; (b) ΔJ_{sc} vs. the optical density of the Si NC layer for different $QE_{Si\ NC}$.

Table 1. Loss processes and Si NC contribution to J_{sc} for the simulated structure.

Loss and gain factors related to Si NC absorption and emission	Contribution to J_{sc} ($mA \cdot cm^{-2}$)
Absorption of NC emission in Si wafer	0.75
Trapping of NC emission	-0.42
Front surface escape + glass abs. of NC emission	-0.25
J_{sc} loss due to NC abs. in high EQE region	-1.03

From Table 1 it becomes apparent that for the simulated structure the major loss factor is the trapping of the Si NC emission in the layer itself. In addition, absorption in the glass coversheet and front surface escape further limit the Si NC emission reaching the cell. Furthermore, a part of the blue-UV irradiation is absorbed in the glass coversheet before it reaches the Si NC layer. If these photons would become available for Si NC absorption this would add 0.04 $mA \cdot cm^2$ to the J_{sc}. The loss in J_{sc} due to Si NC absorption in the solar cell's high EQE wavelength range of 400 – 600 nm is included at the bottom of Table 1. Note that the above J_{sc} calculations were performed using EQE characteristics obtained from the model corresponding to illumination between the solar cell's fingers (open area).

Subsequently, the analysis was extended by variation of the Si NC layer thickness and the $QE_{Si\ NC}$. The variation in layer thickness is used to vary the amount of absorption in the Si NC layer. The range of $QE_{Si\ NC}$ was extended to values above 1. This corresponds to Si NC layers which demonstrate efficient quantum cutting. Currently, no Si NC layers with QE larger than 1 have been reported in literature. With other materials this has been achieved.[11] The results of this analysis are included in Fig. 4b which reports the change in J_{sc} as a function of Si NC layer optical density (OD) at 300 nm incident radiation for different $QE_{Si\ NC}$. From this figure, it is clear that in order to realize gain in J_{sc} for the simulated module structure very high quantum yields of emission are required. In our analysis gain in J_{sc} is seen only from $QE_{Si\ NC} = 1.6$ (not included in the Fig. 4b). Moreover, note that in these simulations a constant $QE_{Si\ NC}$ is assumed over the entire emission range and quantum cutting is generally more efficient at higher excitation energies.

4. Conclusions

We have reported the down-shifting action of a thin film of Si NCs in matrix of SiO_2 on a p-type c-Si solar cell. The proof-of-concept configuration employed here bears close resemblance with the optical stack encountered in a solar module with the Si NCs applied to the inside of the front coversheet. Due to the low $QE_{Si\ NC}$ of the current Si NC sample a reduction of the EQE was observed throughout the Si NC absorption range. Nevertheless, with the help of ray tracing simulations it was shown that down-shifting action is required to explain the observed changes in the EQE. With the ray tracing model loss factors which impact the performance of down-shifting (and down-converting) Si NC layers in a c-Si solar module configuration were identified. These include a low emission coupling efficiency, Si NC absorption in the wavelength range of high solar cell EQE and UV absorption by the glass coversheet. Currently, these loss factors severely impact the performance. It was found that to obtain gain in J_{sc} at module level (with low iron glass and EVA) a very high Si NC emission QE is required (> 1.6), which would correspond to very efficient quantum cutting. In order to facilitate successful incorporation of Si NCs in a c-Si solar module in the configuration studied here further investigations aimed at improvement of the emission coupling efficiency are required.

Acknowledgements

This work is supported by NanoNextNL, a micro and nanotechnology consortium of the Government of the Netherlands and 130 partners. The authors would like to thank N.J. Bakker and T. van den Driesschen for their help in performing the spectral response measurements.

References

[1] Van Sark, WGJHM, Meijerink, A, Schropp, REI, Van Roosmalen, JAM, Lysen, EH. Enhancing solar cell efficiency by using spectral converters, SOL ENERG MAT SOL C. 2005;87:395-409.
[2] Van Sark, WGJHM, De Wild, J, Rath, JK, Meijerink, A, Schropp, REI. Upconversion in solar cells. Nanoscale Res. Lett. 2013;8:81.
[3] Shockley, W, Queisser, HJ., Detailed balance limit of efficiency of p-n junction solar cells, J. Appl Phys 1961;32:510-519.
[4] Timmerman, D, Valenta, J, Dohnalová, K, De Boer, WDAM, Gregorkiewicz, T. Step-like enhancement of luminescence quantum yield of silicon nanocrystals, Nature Nanotech. 2011;6:710-713.
[5]Tuan Trinh, M, Limpens, R, de Boer, WDAM, Schins, JM, Siebbeles, LDA, Gregorkiewicz, T. Direct generation of multiple excitons in adjacent silicon nanocrystals revealed by induced absorption, Nature Phot. 2012;6:316-321.
[6] Ingenhoven, P, Anopchenko, A, Tengattini, A, Gandolfi, D, Sgrignuoli, F, Pucker, G, Jestin, Y, Pavesi, L, Balboni, R. Quantum effect in silicon for photovoltaic applications, Phys. Status Solidi A 2013;210:1071-1075.
[7] Limpens, R, Gregorkiewicz, T. Spectroscopic investigations of dark Si nanocrystals in SiO_2 and their role in external quantum efficiency quenching, J Appl Phys 2013;114:74304.
[8] Burgers, AR, Slooff, LH, Kindeman, R, Van Roosmalen, JAM. Modelling of luminescent concentrators by ray-tracing, Proceedings of 20th EC Photovolt. Solar Ener. Conf 2005:394-397.
[9] Takeoka, S, Fujii, M, Hayashi, S. Size-dependent photoluminescence from surface oxidized Si nanocrystals in a weak confinement regime, Phys. Rev. B 2000;62:16820
[10] McIntosh, KR, Lau, G, Cotsell, JN, Hanton, K, Batzner, DL, Bettiol, F, Richards, BS. Increase in external quantum efficiency of encapsulated silicon solar cells from a luminescent down-shifting layer, Prog. Photovolt.2009;17:191-197
[11] Semonin, OE, Luther, JM, Choi, S, Chen, H-Y, Gao, J, Nozik, AJ, Beard, MC Peak External Photocurrent Quantum Efficiency Exceeding 100% via MEG in a Quantum Dot Solar Cell, Science 2011;334:1530.